

9-2014

The Effect of Tooth Presence on Identification of Tooth Socket Lamina Dura Surface: A CBCT Study

Morse Stonecypher

Follow this and additional works at: <http://scholarsrepository.llu.edu/etd>

 Part of the [Orthodontics and Orthodontology Commons](#), and the [Orthopedics Commons](#)

Recommended Citation

Stonecypher, Morse, "The Effect of Tooth Presence on Identification of Tooth Socket Lamina Dura Surface: A CBCT Study" (2014).
Loma Linda University Electronic Theses, Dissertations & Projects. 206.
<http://scholarsrepository.llu.edu/etd/206>

This Thesis is brought to you for free and open access by TheScholarsRepository@LLU: Digital Archive of Research, Scholarship & Creative Works. It has been accepted for inclusion in Loma Linda University Electronic Theses, Dissertations & Projects by an authorized administrator of TheScholarsRepository@LLU: Digital Archive of Research, Scholarship & Creative Works. For more information, please contact scholarsrepository@llu.edu.

LOMA LINDA UNIVERSITY
School of Dentistry
in conjunction with the
Faculty of Graduate Studies

The Effect of Tooth Presence on Identification
of Tooth Socket Lamina Dura Surface:
A CBCT Study

by

Morse Stonecypher

A thesis submitted in partial satisfaction of
the requirements for the degree
Master of Science in Orthodontics and Dentofacial Orthopedics

September 2014

© 2014

Morse Stonecypher
All Rights Reserved

Each person whose signature appears below certifies that this thesis in his/her opinion is adequate, in scope and quality, as a thesis for the degree of Master of Science.

_____, Chairperson
Kitichai Rungcharassaeng, Professor of Orthodontics and Dentofacial Orthopedics

Joseph Caruso, Professor of Orthodontics and Dentofacial Orthopedics

Joseph Kan, Professor of Restorative Dentistry

ACKNOWLEDGEMENTS

I would like to express my deep appreciation for the faculty members who have helped shape my thesis into something of which I can be proud. First and foremost, I want to express my gratitude to Dr. Kitichai Rungcharassaeng who has guided me through much of process of creating a working protocol and thesis. I am indebted to him for his patient explanations of study design, data collection, and statistical analysis. Second, I would like to acknowledge Dr. Joseph Caruso for his insights and ability to simplify even the most complex of problems. Finally, I want to thank Dr. Joseph Kan for his input, advice, and comments.

I would also like to thank God for giving me the opportunity, drive, and determination to complete my education. All I have and all I am I owe to Him.

CONTENTS

Approval Page.....	iii
Acknowledgements.....	iv
Table of Contents.....	v
List of Tables.....	vi
List of Figures.....	vii
List of Abbreviations.....	viii
Abstract.....	ix
Chapter	
1. Review of the Literature.....	1
2. The Effect of Tooth Presence on Identification of Tooth Socket Lamina Dura Surface: A CBCT Study.....	6
Abstract.....	6
Introduction.....	8
Materials and Methods.....	9
Statistical Analysis.....	16
Results.....	17
Discussion.....	28
Conclusions.....	31
References.....	32
Additional References.....	33

TABLES

Tables	Page
1. List of Extracted Teeth by Head	17
2. Comparison of Identified Coordinates by Time-Point, T1-T2	18
3. Comparison of Identified Coordinates by Time-Point, T1-T3	19
4. Comparison of Identified Coordinates by Time-Point, T2-T3	19
5. Comparison of Absolute Discrepancies of All Time-Points.....	22
6. Comparisons of Absolute Discrepancies in the Maxilla and Mandible, T1-T2	23
7. Comparisons of Absolute Discrepancies in the Maxilla and Mandible, T1-T3	23
8. Comparisons of Absolute Discrepancies in the Maxilla and Mandible, T2-T3	24
9. Comparison of Coordinate Absolute Discrepancy by Bone Level, T1-T2.....	25
10. Comparison of Coordinate Absolute Discrepancy by Bone Level, T1-T3.....	25
11. Comparison of Coordinate Absolute Discrepancy by Bone Level, T2-T3.....	26
12. Specific Comparison of Absolute Discrepancy of FLD and FBS with T3 FBT ...	27

FIGURES

Figures	Page
1. Working Model with Radiographic Template, Oblique View.....	10
2. Working Model with Radiographic Template, Occlusal View	11
3. Example of Volume Superimposition.....	13
4. Constructed Grid in Keynote Presentation Program.....	15
5. Point Placement at 200% Slide Magnification	16
6. Percentage frequency distribution of absolute discrepancy in pixels between T1 and T2.....	20
7. Percentage frequency distribution of absolute discrepancy in pixels between T1 and T3.....	20
8. Percentage frequency distribution of absolute discrepancy in pixels between T2 and T3.....	21

ABBREVIATIONS

CBCT	Cone-Beam Computed Tomography
FBM	Facial Bone Margin
FBS	Facial Bone Surface
FBT	Facial Bone Thickness
FLD	Facial Lamina Dura
FOV	Field of View
LBM	Lingual Bone Margin
LLD	Lingual Lamina Dura
Px	Pixel
SA	Socket Apex
T1	Time-point 1
T2	Time-point 2
T3	Time-point 3

ABSTRACT OF THE THESIS

The Effect of Tooth Presence on Identification of Tooth Socket Lamina Dura Surface: A CBCT Study

by

Morse Stonecypher

Master of Science in Orthodontics and Dentofacial Orthopedics
Loma Linda University, September 2014
Dr. Kitichai Rungcharassaeng, Chairperson

Aim: The accuracy in identifying anatomical landmarks on CBCT images can be affected by the presence of surrounding anatomical structures with similar radiodensity. The purpose of this study was to evaluate the effect of the presence of tooth structure on the accuracy in identifying the lamina dura surface, facial bone surface, facial and lingual bone margins, socket apex, as well as in facial bone thickness measurement. **Materials & Methods:** Three fresh cadaver heads were scanned using a NewTom 5G CBCT at 0.100 mm voxel size at three time-points: before extraction (T1), after extraction and reinsertion (T2), and after tooth removal (T3). Only single rooted teeth were extracted in a minimally traumatic fashion. The volumes were superimposed (Invivo 5.2) in pairs (T1-T2, T1-T3, T2-T3) and mid-sagittal images of each socket were produced. The lamina dura and facial bone surfaces were plotted at 3, 5, 7, 9, and 11 mm apical to the CEJ. In addition, the facial and lingual bone margins, and the socket apex were plotted. The point coordinates were recorded and the facial bone thickness calculated. The discrepancies of all parameters between time-points were compared using Wilcoxon Signed Rank test ($\alpha = 0.05$). **Results:** Although there were statistically significant differences ($p < 0.05$) in time-point discrepancy in 5 of 21 parameters evaluated, the

measured discrepancies were low and likely clinically inconsequential. **Conclusions:** At 0.100 mm voxel size, the ability to accurately identify socket lamina dura, and measure the facial bone thickness on CBCT images does not seem to be clinically affected by the presence of tooth structure, nor by the minimally traumatic extraction procedure.

CHAPTER ONE

REVIEW OF THE LITERATURE

Cone-Beam Computed Tomography (CBCT) has become an instrumental part of diagnostics and treatment planning in dentistry since its introduction to the field in 1998.¹ It is fast becoming the preferred method for evaluation of patients undergoing treatment in oral surgery, periodontics, implant dentistry, and endodontics. It can also be a very useful adjunct in orthodontics.

CBCT is growing in popularity among orthodontists because it gives a 3-dimensional reconstruction of the face, bones, teeth, and airway. Via a single CBCT scan an orthodontist can also reconstruct the traditional 2-dimensional radiographs with high enough precision for diagnostics and treatment planning.² The 2-dimensional reconstruction can also offer detailed views of buccal and lingual cortical plates, something not possible with traditional 2-dimensional radiographs. Since tooth movements in the bucco-lingual direction can cause bony dehiscences and compromise long-term periodontal stability,³ the reliability of CBCT to accurately image these areas of thin bone is important to any orthodontist that uses this modality.

The introduction of CBCT technology to the dental field initiated a surge of research into the physics of CBCT imaging and the algorithms of volume capturing and reconstruction.¹⁹ Through that research, advances in technology have resulted in a decrease in radiation dose per scan and increase in voxel resolution. The overall goal is to produce the most accurate scan with the least radiation possible, and this research has

improved the overall understanding of the accuracy of measurements made in a volume. Since 2004, there has been an exponential increase in research articles dealing with CBCT linear accuracy and its reflection on reality.¹⁹

The earliest studies of CBCT accuracy were based around acrylic phantoms and caliper measurements. Kobayashi et al researched measurements made on a dry mandible and an acrylic block using CBCT and digital calipers, and found high accuracy of measurements.⁴ Various study designs have been created to test accuracy, ranging from acrylic blocks with drilled holes to dry mandibles with simulated bone defects to ex vivo maxillae fixed in formalin and embedded with gutta percha markers.⁵⁻⁷ A project by Sun et al found sub-millimeter accuracy between CBCT and physical caliper measurements on dry skull specimens.⁸ These studies each reported high degrees of accuracy, sub-millimeter correlation, and very little distortion. It is important to note these studies almost exclusively deal with linear measurements over a large distance using phantoms and dry specimens.

Fewer studies look at the spatial resolution of CBCT imaging to determine just how small an increment can be accurately measured, and to date no studies have definitively determined the minimum bone thickness visualized by CBCT. In 2012, Patcas et al discovered that, using the limits of agreement from their study, the discrepancy between CBCT images and physical measurements could be as much as 2 mm of bone thickness, with an average of 1 mm less bone visualized on CBCT when compared to caliper measurements. Should this much bone be missing, there is a high risk of false-positive identification of intrabony dehiscences. Their conclusion was that

soft tissues and other structures were having an effect on the CBCT beam and thus image quality, though they did not speculate on exactly which structures were at fault.¹²

In another study by Menezes et al, researchers embedded dry mandibles in wax and surrounded them with water and detergent to simulate soft tissue density around the bone. The buccal and cortical plates were then measured and compared between three different scan protocols utilizing different voxel sizes (0.3, 0.4, and 0.5 mm voxels). They found that areas of thin bone, especially in the anterior mandible, were difficult to distinguish regardless of the voxel size and had higher inter-observer variation than areas of thicker bone in the posterior mandible.¹⁵ Their results agree with Mol and Balasundaram, who found that mandibular anterior teeth had lower accuracy than other areas.²² These studies emphasize the limitations of spatial resolution in CBCT machines.

Several possible reasons for decreased accuracy of small distance measurements include the anatomic structures of the head and neck, spatial resolution, contrast resolution, head positioning in the machine, FOV, noise, and the embalming of cadavers.

Anatomical structures of the head and neck may interfere with the X-ray beam, and thus reduce the overall quality of a CBCT volume. Possible culprits include the vertebral column, cranial base, facial bones, and soft tissues.²⁰ However, to date the literature shows no definitive link between a specific structure and scans with areas of omitted bone.

It is important to note that CBCT accuracy is also dependent upon certain criteria that can affect the observer's ability to precisely place markers in the software for measurement, such as contrast resolution. Contrast resolution is the ability of the observer to distinguish between different densities. High contrast between the edge of an

object and its surroundings improves the ability of the observer to pick out the boundaries of that object.⁹ Thus, cementum and bone, which have similar radiodensities, would be difficult to distinguish, as compared to cortical bone and air.

Additionally, CBCT machines employ a “partial volume averaging” in which a voxel’s assigned radiodensity is the average of the anatomical structures that it encompasses. The volume averaging of a voxel also a function of spatial resolution: the ability to distinguish between two objects in close proximity. The closer two objects are to each other, the higher the likelihood the voxel will span their boundaries and average the two densities. This becomes especially problematic in areas where bone thickness approaches the maximum spatial resolution of the machine.⁹ Thus, close proximity of structures with similar radiodensities may lead either the observer or the machine to overlook the delineation of objects and see them as one, as opposed to X-ray beam interference from various anatomical structures.

Head positioning in the machine can also affect the visualization of bone. A study by Ahlqvist and Isberg found that variations in apparent bone thickness were found depending on the angle of the X-ray beam to the bone.¹³

FOV and scatter noise are also linked to changes in measured bone. In CBCT imaging, scatter noise increases with increased FOV.¹⁴ Thus, the best images are obtained at the smallest FOV to decrease noise as much as possible.

The embalming process for preserved cadavers is known to shrink tissues, alter tissue architecture, and disrupt periodontal structures.²³⁻²⁶ The use of fresh cadavers in CBCT studies is a good way to avoid this problem and still approximate a true clinical situation.

The aim of this study was to investigate the effect of tooth presence on the ability to identify the socket lamina dura and bone surfaces. The study used fresh cadaver heads to avoid the problems created by preservation and to closely mimic a true clinical setting. Scans were taken before and after extraction, and discrepancies in the delineation of lamina dura and bone surfaces were recorded. The Null Hypothesis was that there would be no significant discrepancies in delineation before or after extraction. The Alternative Hypothesis was that there would be a significant difference.

CHAPTER TWO
THE EFFECT OF TOOTH PRESENCE ON IDENTIFICATION
OF TOOTH SOCKET LAMINA DURA: A CBCT STUDY

Abstract

Aim: The accuracy in identifying anatomical landmarks on CBCT images can be affected by the presence of surrounding anatomical structures with similar radiodensity. The purpose of this study was to evaluate the effect of the presence of tooth structure on the accuracy in identifying the lamina dura surface, facial bone surface, facial and lingual bone margins, socket apex, as well as in facial bone thickness measurement. **Materials & Methods:** Three fresh cadaver heads were scanned using a NewTom 5G CBCT at 0.100 mm voxel size at three time-points: before extraction (T1), after extraction and reinsertion (T2), and after tooth removal (T3). Only single rooted teeth were extracted in a minimally traumatic fashion. The volumes were superimposed (Invivo 5.2) in pairs (T1-T2, T1-T3, T2-T3) and mid-sagittal images of each socket were produced. The lamina dura and facial bone surfaces were plotted at 3, 5, 7, 9, and 11 mm apical to the CEJ. In addition, the facial and lingual bone margins, and the socket apex were plotted. The point coordinates were recorded and the facial bone thickness calculated. The discrepancies of all parameters between time-points were compared using Wilcoxon Signed Rank test ($\alpha = 0.05$). **Results:** Although there were statistically significant differences ($p < 0.05$) in time-point discrepancy in 5 of 21 parameters evaluated, the measured discrepancies were low and likely clinically inconsequential. **Conclusions:** At

0.100 mm voxel size, the ability to accurately identify socket lamina dura, and measure the facial bone thickness on CBCT images does not seem to be clinically affected by the presence of tooth structure, nor by the minimally traumatic extraction procedure.

Introduction

Cone-Beam Computed Tomography has become an instrumental part of diagnostics and treatment planning for various areas in dentistry since its introduction.¹ CBCT is growing in popularity among orthodontists because it gives 3-dimensional views of the face, bones, teeth and airway. A single scan can also render reconstructed 2-dimensional radiographs with high enough quality for orthodontic diagnosis and treatment planning.²

Traditional radiography does not allow for detailed views of the buccal and lingual cortical plates, and excessive orthodontic tooth movement in these directions can trigger dehiscences or compromise long-term periodontal stability.³ CBCT offers the distinct advantage of visualizing these areas of interest, and so the accurate imaging of thin cortical plates becomes important to any orthodontist using CBCT.

High levels of linear accuracy of CBCT have been reported, especially with regard to phantoms, ex vivo maxillas, dry mandibles, and skulls.⁴⁻⁸ However, each of these studies looked at measurements over large distances.⁴⁻⁸ On the other hand, the findings regarding relationship between the CBCT spatial resolution and the minimal distance that can be measured accurately have been inconclusive.⁹ Furthermore, as CBCT machines employ a “partial volume averaging” feature, in which a voxel’s assigned radiodensity is the average of the anatomical structures that it encompasses, the presence of objects with similar radiodensity in close proximity,⁹ ie. tooth/root structure and facial bone, can affect the CBCT measurement accuracy.¹⁰

The purpose of this study was to evaluate the effect of the presence of tooth structure on the accuracy in identifying the lamina dura surface, facial bone surface,

facial and lingual bone margins, socket apex, as well as in measuring facial bone thickness. The Null Hypothesis was that there would be no significant discrepancies in identification before or after extraction. The Alternative Hypothesis was that there would be a significant difference.

Materials and Methods

Three fresh, frozen, dentate cadaver heads were obtained from the Loma Linda University Bodies for Science program. The study was filed but exempted from IRB approval. The heads were first screened using the following criteria:

1. Each head must contain as many teeth as possible, with a minimum of 10 teeth per jaw, which must include at least one molar bilaterally.
2. As few metallic restorations as possible.
3. No or minimal periodontal destruction.
4. No visible structural damage resulting from trauma or pathology in either jaw.

Impressions were made of each arch using irreversible hydrocolloid impression material (Dust-Free Fast-Set Alginate, Dux Dental, California) and casts were fabricated using dental stone (Ortho Stone, Heraeus-Kulzer Inc., Germany). Undercuts on the casts were blocked-out using block-out resin (LC Block-out Resin, Ultradent, Missouri).

A radiographic template was then constructed of 2 mm vacuum-formed plastic (Splint Bioacryl, Great Lakes Orthodontics, New York). Radiopaque 2-3 mm pieces of 18 gauge aluminum wire (Impex System Collaborators, Florida) were fixed to the template with a radiolucent non-filled resin (Adper Scotchbond Multi-Purpose Adhesive,

3M ESPE, Minnesota) at the incisal tip, the free gingival margin, and the deepest edge of the template (Figures 1, 2). The radiographic template was intended to be used as guide for image superimposition in three dimensions for analysis, and was used in all CBCT scans.



Figure 1: Working model with radiographic template, oblique view. Aluminum markers are present at the approximate incisal tip, gingival margin, and deepest vestibular margin.



Figure 2: Working model with radiographic template, occlusal view. Note that the plastic wraps around the occlusal/incisal surfaces of the teeth for stability and to hold the extracted teeth in place.

The scans were performed using a NewTom 5G CBCT machine (QR S.r.l., Verona, Italy). Volumes were captured using 0.100 mm voxel size, 12x8 cm field-of-view (FOV), 110 kV, 4.19-14.87 mA (varying according to the size of the head), and 5.4 s scan time. A preliminary scan was performed before any alteration to the teeth or tissues (T1).

Single rooted teeth were selected for extraction to minimize the damage to the surrounding alveolar bone and to minimize the chance of root fracture. First premolars and all existing molars were not extracted and used to provide support and stability to the template.

Extractions were performed using a Periotome instrument (Nobel Biocare, Yorba Linda, California), periosteal elevators, and extraction forceps. The supracrestal gingival

attachment was carefully severed to preserve the gingiva. Luxation was performed with a Periosteal instrument followed by extraction forceps. Teeth were luxated until they could be removed from the socket, at which point they were reinserted into the alveolus with finger pressure (T2). The teeth were held in position by the radiographic template and the T2 scan performed. Subsequently, the luxated teeth were gently removed with extraction forceps (T3). The radiographic template was then reinserted and the final scan taken (T3).

The CBCT volumes were superimposed three-dimensionally in pairs (T1-T2, T1-T3, and T2-T3) using Invivo software (Anatomage, v.5.2, San Jose, California). During superimpositions, discrepancies were noted between the position of the radiographic markers and hard tissue landmarks, so the final/precise superimpositions were performed manually using hard tissue landmarks such as ANS, the malar prominences, the floor of the maxillary sinuses, roots of non-extracted teeth, the mandibular symphysis, the mandibular cortical plates, etc. (Figure 3). All superimpositions were performed by a single examiner (MS).

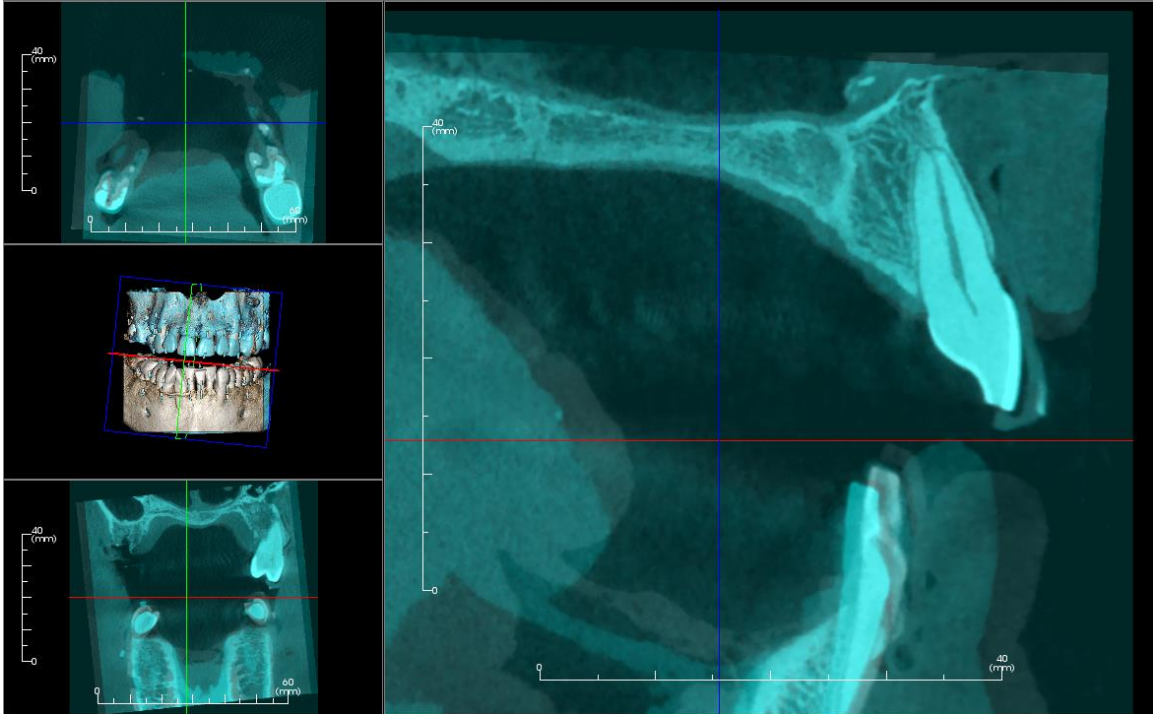


Figure 3: Example of volume superimposition. T1-T2 superimposition of the maxillary right central incisor, Sagittal Cut, MPR View. Bony superimposition was prioritized, and each jaw was independently superimposed.

Mid-sagittal images of each tooth-socket combination, along the long axis of the tooth, were produced. The paired-images were zoomed in to a factor of 1:2.68 (40 mm Anatomage ruler occupied 107 mm on screen). Each image was then screen captured and imported into the Keynote presentation program (v.9.3, Apple Inc., California) for analysis as in Roe et al.¹¹ The images were not further resized. The length of the Anatomage ruler (40 mm) was recorded as 470 pixels on the Keynote slide, which translated to 0.085 mm per pixel. The first paired-image was then orientated until the line connecting facial and lingual CEJs (CEJ Line) became horizontal. The angular change of the image was recorded and used to orientate the second paired-image. The X-

Y coordinates of the Anatomage rulers on both pair-images were matched to ensure no discrepancies existed.

A grid was superimposed on the first paired-image with the following lines: 1) the horizontal CEJ Line, 2) a vertical reference line perpendicular to the CEJ line, and 3) the Level Lines parallel and at 3, 5, 7, 9 and 11 mm apical to the CEJ Line (Level Lines 1-5, respectively; Figure 4). Lingual lamina dura (LLD), facial lamina dura (FLD), and facial bone surface (FBS) were identified with single pixel points along the Level Lines. The coordinates were recorded and the time-point discrepancies calculated in horizontal plane using X-axis coordinates. Facial bone thickness (FBT) at each Level Line was the difference between FBS and FLD X-axis coordinates and expressed in pixels. Lingual bone margin (LBM), facial bone margin (FBM), and socket apex (SA) were also identified, but the discrepancies were calculated in the vertical plane using Y-axis coordinates (Figure 5). The discrepancies in the X-axis were given a positive value when the second time-point moved away from the socket, and a negative value was given to discrepancies moving toward the socket. Discrepancies in the Y-axis were given a positive value when the second time-point moved coronal, negative when it moved apical. These discrepancies were recorded as directional discrepancies, which were subsequently converted to absolute values and recorded as absolute discrepancies. All point placements were performed by a single examiner (MS) in Keynote at 200% slide magnification (Figure 4), where pixel size remained constant at 0.085 mm. The landmark identifications were performed first on the image of the earlier time-point of the paired-images (ie. T1 before T2/T3 and T2 before T3). Areas with visible damage after luxation/extraction were excluded from the analysis.



Figure 4: Constructed grid in Keynote presentation program. The image was rotated to match the buccal and lingual CEJs with the horizontal CEJ Line.

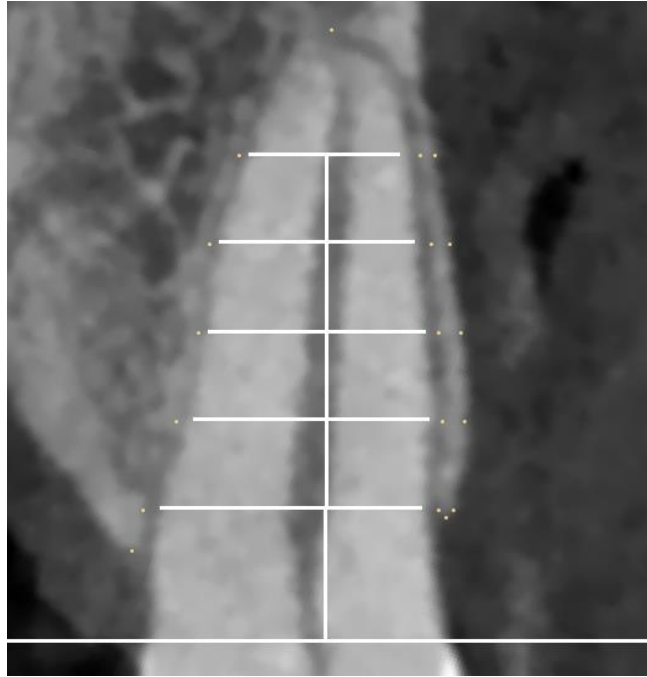


Figure 5: Point placement at 200% slide magnification. Each yellow dot represents a single pixel. The examiner used these dots to plot the LLD, FLD, FBS, LBM, FBM, and SA (all pictured). In cases where the bone margin was >3 mm from the CEJ line, the X-axis points at the 3 mm mark were discarded.

Statistical Analysis

The intra- and inter-examiner reliabilities of the method were determined by using triple assessments of each parameter by 2 examiners (MS and EC) on 10 randomly selected paired-images made at least 2 weeks apart and expressed as the intraclass correlation coefficients (ICC). Means and standard deviations of both directional and absolute discrepancies were calculated for each parameter. Only absolute discrepancy data were analyzed statistically using Spearman's Rank Correlation analysis, Wilcoxon Signed Rank, Kruskal-Wallis, Mann-Whitney U, and Friedman's Two-Way Analysis of Variance by Ranks Tests. The significance level of $\alpha = 0.05$ was used for all statistical analyses.

Results

A total of 38 (20 maxillary and 18 mandibular) teeth and their respective sockets were evaluated in this study. The tooth distribution is shown in Table 1.

Table 1. List of Extracted Teeth by Head.

Tooth	Head 1	Head 2	Head 3	Total
Mx Central	2	2	2	6
Mx Lateral	2	1	1	4
Mx Canine	1	2	2	5
Mx 2 nd Premolar	1	2	2	5
Md Central	2	1	0	3
Md Lateral	0	2	1	3
Md Canine	2	2	2	6
Md 2 nd Premolar	2	2	2	6
Total	12	14	12	38

ICC values were very high for both intra-examiner ($r \geq 0.993$), and inter-examiner ($r \geq 0.986$) data, indicating that the identification methods were reliable and reproducible. Tables 2-4 display the means and standard deviations of both directional and absolute time-point discrepancies of all parameters. They ranged from -0.56 ± 1.99 px (-0.048 ± 0.169 mm) to 1.08 ± 2.16 px (0.092 ± 0.184 mm) for directional and 0.69 ± 0.70 px (0.058 ± 0.060 mm) to 1.79 ± 1.93 px (0.152 ± 0.165 mm) for absolute time-point discrepancies. The identified coordinates between time-points (values not shown) were compared using Wilcoxon Signed Rank Test, and correlated using Spearman's Rho at $\alpha = 0.05$. There were no statistically significant differences found between T1 and T2 coordinates ($p > 0.05$; Table 2). Significant differences were found in LLD, FBS, and

FBT between T1 and T3 coordinates ($p < 0.05$; Table 3); and in FLD and FBT between T2 and T3 coordinates ($p < 0.05$; Table 4). All paired coordinates were highly correlated ($r > 0.90$, $p < 0.01$; Tables 2-4). Frequency distributions of absolute discrepancy in pixels between time-points are exhibited in Figures 6-8.

Table 2: Directional and absolute time-point discrepancies between T1 and T2. Identified coordinates by time-point (values not shown) were compared using Wilcoxon Signed Rank Test, and correlated using Spearman's Rho at $\alpha = 0.05$.

Parameter	N	Time-point Discrepancy (T1-T2)		T1 vs. T2		
		Mean \pm SD in pixel [mm]		Wilcoxon p-value	Spearman's Rho	
		Directional	Absolute		r-value	p-value
LLD	157	-0.11 \pm 1.75 [-0.010 \pm 0.149]	1.17 \pm 1.30 [0.100 \pm 0.110]	0.649	1.000	0.000
FLD	124	0.16 \pm 1.19 [0.014 \pm 0.101]	0.90 \pm 0.79 [0.076 \pm 0.067]	0.153	1.000	0.000
FBS	124	0.12 \pm 1.23 [0.010 \pm 0.104]	0.86 \pm 0.88 [0.073 \pm 0.075]	0.209	1.000	0.000
FBT	124	0.05 \pm 1.66 [0.004 \pm 0.141]	1.02 \pm 1.31 [0.086 \pm 0.111]	0.930	0.918	0.000
LBM	38	-0.05 \pm 2.56 [-0.004 \pm 0.218]	1.63 \pm 1.95 [0.139 \pm 0.166]	0.342	0.999	0.000
FBM	34	0.18 \pm 1.88 [0.015 \pm 0.160]	1.24 \pm 1.42 [0.105 \pm 0.120]	0.314	0.999	0.000
SA	38	0.32 \pm 1.58 [0.027 \pm 0.134]	1.05 \pm 1.21 [0.090 \pm 0.103]	0.424	0.999	0.000

Table 3: Directional and absolute time-point discrepancies between T1 and T3. Identified coordinates by time-point (values not shown) were compared using Wilcoxon Signed Rank Test, and correlated using Spearman’s Rho at $\alpha = 0.05$.

Parameter	N	Time-point Discrepancy (T1-T3)		T1 vs. T3		
		Mean \pm SD in pixel [mm]		Wilcoxon p-value	Spearman’s Rho	
		Directional	Absolute		r-value	p-value
LLD	157	-0.27 \pm 1.65 [-0.023 \pm 0.140]	1.08 \pm 1.27 [0.092 \pm 0.108]	0.024*	0.999	0.000
FLD	124	-0.21 \pm 1.24 [-0.018 \pm 0.106]	0.90 \pm 0.88 [0.076 \pm 0.075]	0.129	0.999	0.000
FBS	124	0.22 \pm 1.33 [0.019 \pm 0.113]	0.96 \pm 0.94 [0.082 \pm 0.080]	0.024*	1.000	0.000
FBT	124	0.43 \pm 1.44 [0.036 \pm 0.123]	1.02 \pm 1.10 [0.087 \pm 0.094]	0.001*	0.948	0.000
LBM	38	-0.11 \pm 2.65 [-0.009 \pm 0.225]	1.79 \pm 1.93 [0.152 \pm 0.165]	0.627	0.999	0.000
FBM	34	-0.53 \pm 2.29 [-0.045 \pm 0.195]	1.47 \pm 1.81 [0.125 \pm 0.154]	0.748	0.999	0.000
SA	38	1.08 \pm 2.16 [0.092 \pm 0.184]	1.76 \pm 1.63 [0.150 \pm 0.139]	0.874	0.999	0.000

* Statistically significant difference.

Table 4: Directional and absolute time-point discrepancies between T2 and T3. Identified coordinates by time-point (values not shown) were compared using Wilcoxon Signed Rank Test, and correlated using Spearman’s Rho at $\alpha = 0.05$.

Parameter	N	Time-point Discrepancy (T2-T3)		T2 vs. T3		
		Mean \pm SD in pixel [mm]		Wilcoxon p-value	Spearman’s Rho	
		Directional	Absolute		r-value	p-value
LLD	157	0.03 \pm 1.55 [0.003 \pm 0.132]	1.13 \pm 1.05 [0.096 \pm 0.090]	0.947	0.999	0.000
FLD	124	-0.39 \pm 1.43 [-0.033 \pm 0.122]	1.05 \pm 1.05 [0.089 \pm 0.089]	0.001*	1.000	0.000
FBS	124	-0.02 \pm 0.98 [-0.002 \pm 0.084]	0.69 \pm 0.70 [0.058 \pm 0.060]	0.858	1.000	0.000
FBT	124	0.35 \pm 1.58 [0.030 \pm 0.135]	1.19 \pm 1.09 [0.102 \pm 0.093]	0.004*	0.910	0.000
LBM	38	-0.18 \pm 1.98 [-0.016 \pm 0.169]	1.24 \pm 1.55 [0.105 \pm 0.132]	0.517	0.998	0.000
FBM	34	-0.56 \pm 1.99 [-0.048 \pm 0.169]	1.38 \pm 1.52 [0.118 \pm 0.129]	0.850	0.999	0.000
SA	38	0.55 \pm 1.74 [0.047 \pm 0.148]	1.34 \pm 1.21 [0.114 \pm 0.103]	0.971	0.999	0.000

* Statistically significant difference.

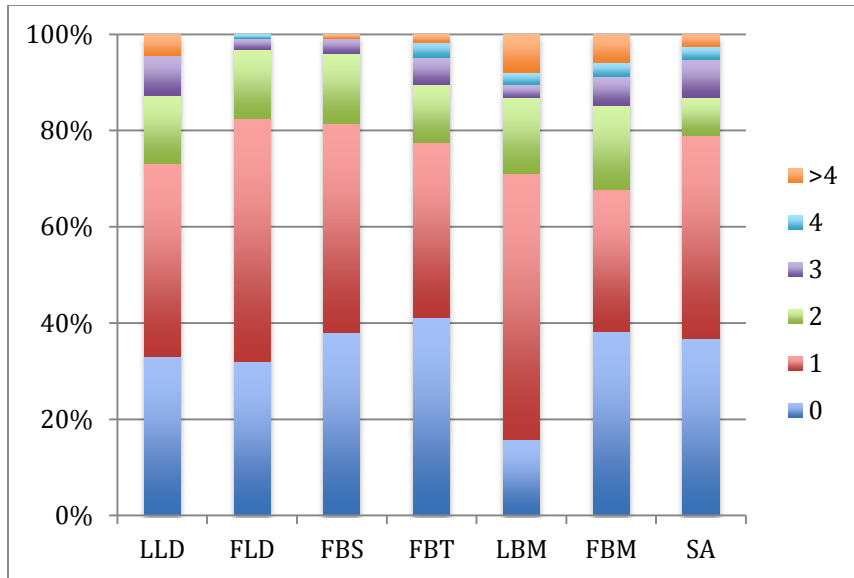


Figure 6: Percentage frequency distribution of absolute discrepancy in pixels between T1 and T2.

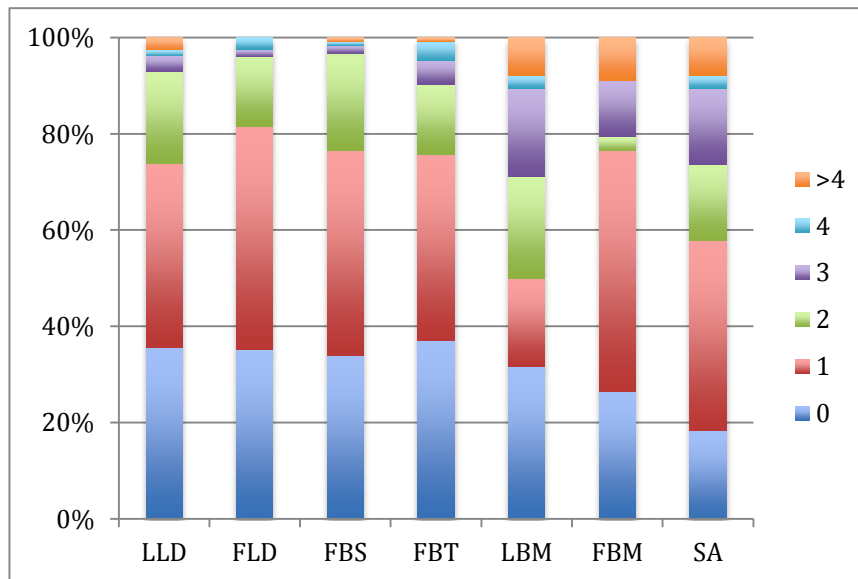


Figure 7: Percentage frequency distribution of absolute discrepancy in pixels between T1 and T3.

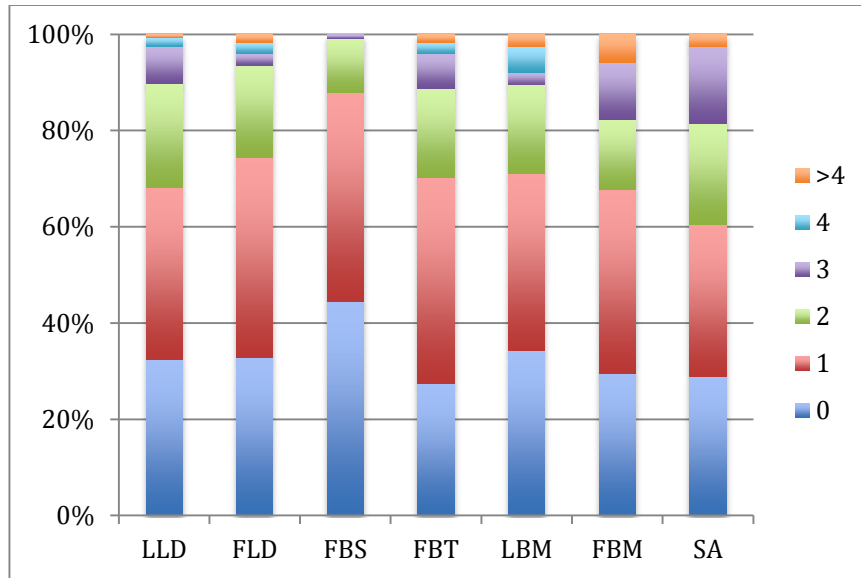


Figure 8: Percentage frequency distribution of absolute discrepancy in pixels between T2 and T3.

Table 5 depicts the comparison of absolute time-point discrepancies among the paired-images of all parameters using Friedman's 2-way ANOVA by Ranks at $\alpha = 0.05$. There were no statistically significant differences found in any of the parameters ($p > 0.05$; Table 5).

Table 5: Comparison of all absolute time-point discrepancies using Friedman's Two-Way Analysis of Variance by Ranks at $\alpha = 0.05$. Pairwise comparisons were performed using Bonferroni Method of Multiple Comparisons.

Parameter	N	Absolute Time-point Discrepancy			p-value
		Mean \pm SD in pixel [mm]			
		T1-T2	T1-T3	T2-T3	
LLD	157	1.17 \pm 1.30 [0.100 \pm 0.110]	1.08 \pm 1.27 [0.092 \pm 0.108]	1.13 \pm 1.05 [0.096 \pm 0.090]	0.561
FLD	124	0.90 \pm 0.79 [0.076 \pm 0.067]	0.90 \pm 0.88 [0.076 \pm 0.075]	1.05 \pm 1.05 [0.089 \pm 0.089]	0.350
FBS	124	0.86 \pm 0.88 [0.073 \pm 0.075]	0.96 \pm 0.94 [0.082 \pm 0.080]	0.69 \pm 0.70 [0.058 \pm 0.060]	0.057
FBT	124	1.02 \pm 1.31 [0.086 \pm 0.111]	1.02 \pm 1.10 [0.087 \pm 0.094]	1.19 \pm 1.09 [0.102 \pm 0.093]	0.158
LBM	38	1.63 \pm 1.95 [0.139 \pm 0.166]	1.79 \pm 1.93 [0.152 \pm 0.165]	1.24 \pm 1.55 [0.105 \pm 0.132]	0.136
FBM	34	1.24 \pm 1.42 [0.105 \pm 0.120]	1.47 \pm 1.81 [0.125 \pm 0.154]	1.38 \pm 1.52 [0.118 \pm 0.129]	0.719
SA	38	1.05 \pm 1.21 [0.090 \pm 0.103]	1.76 \pm 1.63 [0.150 \pm 0.139]	1.34 \pm 1.21 [0.114 \pm 0.103]	0.105

Tables 6-8 compare the absolute time-point discrepancy between Maxillary and Mandibular data using Mann-Whitney U Test at $\alpha = 0.05$. Significant differences were found in SA between T1 and T2 coordinates ($p = .002$; Table 8); and in LLD between T1 and T3 coordinates ($p = .026$; Table 9).

Table 6: Comparison of T1-T2 absolute time-point discrepancy between Maxillary and Mandibular teeth using Mann-Whitney U Test at $\alpha = 0.05$.

Parameter	Absolute Time-point Discrepancy (T1-T2)		p-value
	Mean \pm SD in pixel [mm]		
	Maxilla	Mandible	
LLD	1.20 \pm 1.30 [0.102 \pm 0.110]	1.14 \pm 1.31 [0.097 \pm 0.111]	0.835
FLD	0.90 \pm 0.76 [0.076 \pm 0.065]	0.90 \pm 0.83 [0.076 \pm 0.071]	0.877
FBS	0.73 \pm 0.69 [0.062 \pm 0.059]	1.02 \pm 1.03 [0.087 \pm 0.088]	0.181
FBT	0.92 \pm 1.01 [0.079 \pm 0.086]	1.12 \pm 1.58 [0.095 \pm 0.134]	0.911
LBM	2.05 \pm 2.33 [0.174 \pm 0.198]	1.17 \pm 1.34 [0.099 \pm 0.114]	0.126
FBM	1.11 \pm 1.37 [0.094 \pm 0.117]	1.40 \pm 1.50 [0.119 \pm 0.128]	0.537
SA	0.54 \pm 0.58 [0.046 \pm 0.050]	1.93 \pm 1.49 [0.164 \pm 0.127]	0.002*

*Statistically significant difference.

Table 7: Comparison of T1-T3 absolute time-point discrepancy between Maxillary and Mandibular teeth using Mann-Whitney U Test at $\alpha = 0.05$.

Parameter	Absolute Time-point Discrepancy (T1-T3)		p-value
	Mean \pm SD in pixel [mm]		
	Maxilla	Mandible	
LLD	0.81 \pm 0.84 [0.069 \pm 0.072]	1.35 \pm 1.56 [0.115 \pm 0.133]	0.026*
FLD	0.84 \pm 0.81 [0.071 \pm 0.069]	0.97 \pm 0.97 [0.082 \pm 0.081]	0.527
FBS	0.83 \pm 0.76 [0.071 \pm 0.064]	1.10 \pm 1.10 [0.094 \pm 0.094]	0.219
FBT	0.89 \pm 0.93 [0.076 \pm 0.079]	1.17 \pm 1.26 [0.100 \pm 0.107]	0.344
LBM	1.80 \pm 2.31 [0.153 \pm 0.196]	1.78 \pm 1.50 [0.151 \pm 0.126]	0.613
FBM	1.37 \pm 2.14 [0.116 \pm 0.182]	1.60 \pm 1.35 [0.136 \pm 0.115]	0.179
SA	1.42 \pm 1.02 [0.121 \pm 0.087]	2.36 \pm 2.27 [0.201 \pm 0.194]	0.410

*Statistically significant difference.

Table 8: Comparison of T2-T3 absolute time-point discrepancy between Maxillary and Mandibular teeth using Mann-Whitney U Test at $\alpha = 0.05$.

Parameter	Absolute Time-point Discrepancy (T2-T3)		p-value
	Mean \pm SD in pixel [mm]		
	Maxilla	Mandible	
LLD	1.11 \pm 1.043 [0.095 \pm 0.089]	1.14 \pm 1.07 [0.097 \pm 0.091]	0.876
FLD	1.24 \pm 1.20 [0.105 \pm 0.102]	0.83 \pm 0.80 [0.070 \pm 0.068]	0.075
FBS	0.68 \pm 0.64 [0.058 \pm 0.054]	0.69 \pm 0.78 [0.059 \pm 0.066]	0.773
FBT	1.21 \pm 1.20 [0.103 \pm 0.102]	1.17 \pm 0.98 [0.100 \pm 0.083]	0.806
LBM	0.95 \pm 1.00 [0.081 \pm 0.085]	1.56 \pm 0.98 [0.132 \pm 0.168]	0.443
FBM	1.37 \pm 1.46 [0.116 \pm 0.124]	1.40 \pm 1.64 [0.119 \pm 0.139]	0.918
SA	1.38 \pm 1.31 [0.117 \pm 0.112]	1.29 \pm 1.07 [0.109 \pm 0.091]	1.000

Tables 9-11 compare the absolute time-point discrepancy among different bone levels using Kruskal-Wallis Test at $\alpha = 0.05$. The only significant difference was found in FLD between T1 and T2 coordinates ($p = 0.014$; Table 9)

Table 9: Comparison of T1-T2 absolute time-point discrepancy among different bone levels using Kruskal-Wallis Test at $\alpha = 0.05$.

Parameter	Absolute Time-point Discrepancy (T1-T2)					p-value
	Mean \pm SD in pixel [mm]					
	Level 1	Level 2	Level 3	Level 4	Level 5	
LLD	1.24 \pm 1.34 [0.105 \pm 0.114]	0.89 \pm 1.01 [0.076 \pm 0.086]	1.19 \pm 1.15 [0.101 \pm 0.098]	0.97 \pm 0.94 [0.083 \pm 0.080]	1.69 \pm 1.91 [0.144 \pm 0.163]	0.505
FLD	0.54 \pm 0.66 [0.046 \pm 0.056]	1.12 \pm 0.82 [0.095 \pm 0.070]	1.13 \pm 0.82 [0.096 \pm 0.069]	0.65 \pm 0.75 [0.056 \pm 0.063]	0.73 \pm 0.70 [0.062 \pm 0.060]	0.014*
FBS	1.23 \pm 1.36 [0.105 \pm 0.116]	0.94 \pm 0.75 [0.080 \pm 0.064]	0.81 \pm 0.83 [0.069 \pm 0.071]	0.76 \pm 0.93 [0.065 \pm 0.079]	0.73 \pm 0.70 [0.062 \pm 0.060]	0.583
FBT	1.31 \pm 1.32 [0.111 \pm 0.112]	1.15 \pm 1.77 [0.098 \pm 0.151]	1.03 \pm 1.05 [0.088 \pm 0.089]	1.08 \pm 1.32 [0.092 \pm 0.112]	0.55 \pm 0.596 [0.046 \pm 0.051]	0.387

*Statistically significant difference.

Table 10: Comparison of T1-T3 absolute time-point discrepancy among different bone levels using Kruskal-Wallis Test at $\alpha = 0.05$.

Parameter	Absolute Time-point Discrepancy (T1-T3)					p-value
	Mean \pm SD in pixel [mm]					
	Level 1	Level 2	Level 3	Level 4	Level 5	
LLD	0.95 \pm 0.921 [0.081 \pm 0.078]	0.86 \pm 0.93 [0.073 \pm 0.079]	0.95 \pm 0.85 [0.081 \pm 0.072]	1.09 \pm 1.22 [0.093 \pm 0.103]	1.59 \pm 2.08 [0.135 \pm 0.177]	0.737
FLD	0.85 \pm 0.69 [0.072 \pm 0.059]	1.00 \pm 1.00 [0.085 \pm 0.085]	0.84 \pm 0.86 [0.071 \pm 0.073]	0.81 \pm 0.90 [0.069 \pm 0.076]	0.95 \pm 0.844 [0.081 \pm 0.072]	0.914
FBS	1.08 \pm 0.862 [0.092 \pm 0.073]	1.09 \pm 1.01 [0.093 \pm 0.086]	0.87 \pm 0.81 [0.074 \pm 0.069]	0.76 \pm 0.72 [0.065 \pm 0.062]	1.05 \pm 1.25 [0.089 \pm 0.107]	0.740
FBT	1.00 \pm 1.00 [0.085 \pm 0.095]	1.12 \pm 0.99 [0.095 \pm 0.084]	0.94 \pm 1.12 [0.080 \pm 0.096]	0.80 \pm 1.04 [0.068 \pm 0.089]	2.85 \pm 1.35 [0.108 \pm 0.115]	0.504

Table 11: Comparison of T2-T3 absolute time-point discrepancy among different bone levels using Kruskal-Wallis Test at $\alpha = 0.05$.

Parameter	Absolute Time-point Discrepancy (T2-T3)					p-value
	Mean \pm SD in pixel [mm]					
	Level 1	Level 2	Level 3	Level 4	Level 5	
LLD	1.19 \pm 1.29 [0.101 \pm 0.110]	0.97 \pm 1.00 [0.083 \pm 0.085]	1.16 \pm 1.04 [0.099 \pm 0.089]	1.26 \pm 1.08 [0.108 \pm 0.092]	1.07 \pm 0.96 [0.091 \pm 0.082]	0.827
FLD	1.15 \pm 0.80 [0.098 \pm 0.068]	1.18 \pm 1.26 [0.101 \pm 0.107]	0.97 \pm 1.14 [0.082 \pm 0.097]	1.04 \pm 0.92 [0.088 \pm 0.078]	0.91 \pm 0.87 [0.077 \pm 0.074]	0.769
FBS	0.77 \pm 0.83 [0.065 \pm 0.071]	0.52 \pm 0.71 [0.044 \pm 0.061]	0.90 \pm 0.75 [0.077 \pm 0.064]	0.68 \pm 0.63 [0.058 \pm 0.053]	0.59 \pm 0.59 [0.050 \pm 0.050]	0.223
FBT	1.62 \pm 0.96 [0.137 \pm 0.082]	1.09 \pm 1.18 [0.093 \pm 0.101]	1.29 \pm 1.01 [0.110 \pm 0.086]	1.28 \pm 1.17 [0.109 \pm 0.100]	0.86 \pm 1.04 [0.073 \pm 0.088]	0.149

The correlations of absolute time-point discrepancy of FLD and FBS with T3 FBT were analyzed using Spearman's Rho at $\alpha = 0.05$ (Table 12). All correlation coefficients were low, and not statistically significant ($p > 0.05$; Table 12)

Table 12: Correlation of absolute time-point discrepancy of FLD and FBS with T3 FBT using Spearman's Rho at $\alpha = 0.05$.

	Time-point	r-value	p-value
FLD Absolute Time-point Discrepancy vs. T3 FBT	T1-T3	0.165	0.067
	T2-T3	0.148	0.102
FBS Absolute Time-point Discrepancy vs. T3 FBT	T1-T3	-0.068	0.455
	T2-T3	-0.017	0.855

Discussion

The accuracy of CBCT output is affected by multiple factors, which include contrast resolution, partial volume averaging, object position in the FOV, FOV size, noise, and beam interference from head and neck structures.^{9,12-14} While linear accuracy of CBCT is fairly well established,⁴⁻⁸ the accuracy of spatial resolution is not well understood.^{12,15}

It is recognized that the spatial resolution of a CBCT volume is affected by the partial volume averaging effect, which tends to blur the delineation of objects with similar density.⁹ Moreover, objects in close proximity with similar radiodensity, such as cementum and lamina dura, tend to become increasingly more difficult to distinguish as the bone thickness, as well as the separation of the objects, approaches the voxel size.^{11,16,17} This study did not attempt to compare the CBCT and physical measurements, but rather to assess the effect of the cementum-bone interface on the accuracy of landmark identification through the superimposition of paired-images with and without the tooth in proximity to the bone. This, in turn, would provide more information on the limit of the spatial resolution.

Even though the results of this study were reported in both directional and absolute values, only absolute values were used for statistical analysis. This is because absolute values amplify the discrepancies between time-points, whereas directional data tend to minimize them.

The results of our study show that the identified coordinates of all parameters within the paired-images were highly correlated ($r \geq 0.910$, $p < .001$; Tables 2-4); and most (16 of 21 parameters) differences were not statistically significant (Tables 2-4).

Furthermore, the mean discrepancy of the parameters with significant differences ranged from -0.39 to 0.43 px (-0.033 to 0.036 mm) and 0.96 to 1.19 px (0.082 to 0.102 mm) for directional and absolute discrepancies, respectively (Tables 3-4). These discrepancies are (extremely) low and likely inconsequential clinically. These results indicate that the presence of the tooth structure seems to have no clinically relevant effect on the identification of lamina dura and bone surfaces.

Frequency distribution of data shows the majority of absolute time-point discrepancies are within 2 px (0.170 mm) [Figures 6-8]. It is worthwhile to note that the percentage of ≤ 2 px absolute time-point discrepancy of the horizontal components (LLD, FLD, FBS and FBT) ranged from 87-97%, whereas that of vertical components (LBM, FBM and SA) ranged from 71-89% (Figures 6-8). The corresponding ranges for percentage of ≤ 3 px absolute time-point discrepancy were 95-100% and 89-97% respectively. This is substantiated by the trend for greater vertical (bone height) discrepancies than horizontal (bone thickness) discrepancies between caliper and CBCT measurements reported in the literature.^{11,16,17} It is believed to be the result of both cortical plates thinning beyond the spatial resolution of the CBCT scan and the close proximity of the tooth root and cementum, thus increasing the difficulty of visualizing the limits of the bone.^{11,16,17} In this study, while there was greater variability in the vertical dimension landmark identification, it is important to note the lack of statistical significant differences in time-point discrepancy for these parameters (Tables 2-4).

Extraction procedures involve severing of dento-gingival fibers, periodontal ligaments, and separation of the tooth from the bony socket. Traditional extraction procedures tend to rely on alveolar compression and cortical plate flexion during luxation

to allow severing of the periodontal fibers.¹⁸ Additionally, trauma from extraction can cause socket expansion and bone movement especially around the facial marginal bone where the bone is usually thin. In this study, the absolute time-point discrepancies among the paired-images were not significantly different from each other ($p > 0.05$; Table 5). These results suggest that minimally traumatic extraction with periotome has no significant effect on the position of socket lamina dura.

In 2013, Wood et al, in an animal study, reported inferior CBCT measurement accuracy in maxilla when compared to the mandible.¹⁰ They attributed the difference to the presence of the thicker and denser cortical bone in the mandible, which provided a greater contrast resolution than the thinner and less dense maxillary trabecular bone.¹⁰ In this study, only 2 of 21 parameters (T1-T2 SA and T1-T3 LLD) showed statistically significant differences when comparing absolute time-point discrepancy between the maxilla and mandible with, interestingly, greater discrepancy in the mandible (Tables 6-8). Nevertheless, the differences of the mean discrepancy were small (1.39 px [0.118 mm] for T1-T2 SA and 0.54 px [0.046 mm] for T1-T3 LLD, $p < 0.05$; Table 6-7) and likely not clinically significant. These results imply that, in the presence of tooth structure, the ability to accurately identify the socket lamina dura is not affected by the type of surrounding bone.

Bone thickness is a factor of interest when evaluating CBCT accuracy. It is logical to think that thicker bone would allow for easier outline/landmark identification and is less prone to change when subjected to trauma from extraction. Bone thickness varies along the root/socket length. Therefore, the effect of bone thickness can be assessed by the degree of difference in discrepancy recorded at different bone levels.

When comparing absolute time-point discrepancy among different bone levels, only T1-T2 FLD showed a statistically significant difference ($p = .014$; Table 9-11) with the difference in mean discrepancy ranging from 0.01 to 0.59 px (0.001 to 0.050 mm). This indicates that the accuracy of landmark identification is not significantly affected by location along the root length or the bone thickness. The lack of association between the accuracy in landmark identification and bone thickness is further substantiated by the extremely weak correlations of absolute time-point discrepancy of FLD and FBS with T3 FBT ($|r| \leq 0.165$; $p > 0.05$; Table 12).

Conclusions

Within the limits of this study, the following conclusions could be made:

1. At 0.1 mm voxel size CBCT scan, the presence of tooth structure did not affect the accuracy in identifying lamina dura and other surrounding bony landmarks.
2. There was more variability in identification of vertical (bone margins and socket apex) than horizontal (lamina dura and bone surface) landmarks.
3. The minimally traumatic Periotome extraction appeared to have no significant effect on the position of the lamina dura.
4. There were no clinically significant differences in time-point discrepancy between the maxilla and the mandible, indicating that the type of bone (cortical or trabecular) was not influencing the ability to identify bony landmarks.
5. There was no association between bone thickness and the accuracy of horizontal (lamina dura and bone surface) landmark identification.

REFERENCES

1. Mozzo P, Procacci C, Tacconi A, Martini PT, Andreis IA. "A new volumetric CT machine for dental imaging based on the cone-beam technique: preliminary results." *Eur Radiol* 1998; 8:1558-1564.
2. Lamichane M, Anderson NK, Rigali PH, Seldin EB, Will LA. "Accuracy of reconstructed images from cone-beam computed tomography scans." *Am J Orthod Dentofacial Orthop* 2009; 136(2):156.e1-e6.
3. Wehrbein H, Bauer W, Diedrich P. "Mandibular incisors, alveolar bone, and symphysis after orthodontic treatment. A retrospective study." *Am J Orthod Dentofacial Orthop* 1996; 110(3):239-246.
4. Kobayashi K, Shimoda S, Nakagawa Y, Yamamoto A. "Accuracy in measurement of distance using limited cone-beam computerized tomography." *Int J Oral Maxillofac Implants* 2004; 19:228-231.
5. Marmulla R, Wortche R, Muhling J, Hassfeld S. "Geometric accuracy of the NewTom 9000 cone beam CT." *Dentomaxillofac Radiol* 2005; 34:28-31.
6. Pinsky HM, Dyda S, Pinsky RW, Misch KA, Sarment DP. "Accuracy of three-dimensional measurements using cone-beam CT." *Dentomaxillofac Radiol* 2006; 35:410-416.
7. Loubele M, Guerrero ME, Jacobs R, Suetens P, van Steenberghe D. "A comparison of jaw dimensional and quality assessments of bone characteristics with cone-beam CT, spiral tomography, and multi-slice spiral CT." *Int J Oral Maxillofac Implants* 2007; 22:446-454.
8. Damstra J, Fourie Z, Huddleston-Slater JJR, Ren Y. "Accuracy of linear measurements from cone-beam computed tomography-derived surface models of different voxel sizes." *Am J Orthod Dentofacial Orthop* 2010; 137:16.e1-e6.
9. Molen AD. "Considerations in the use of cone-beam computed tomography for buccal bone measurements." *Am J Orthod Dentofacial Orthop* 2010; 137(4, Suppl):S130-135.
10. Wood R, Sun Z, Chaudhry J, Tee BC, Kim DG, et al. "Factors affecting the accuracy of buccal alveolar bone height measurements from cone-beam computed tomography images." *Am J Orthod Dentofacial Orthop* 2013; 143(3):353-364.

11. Roe P, Kan JYK, Rungcharassaeng K, Caruso JM, Zimmerman G, et al. "Horizontal and vertical dimensional changes of peri-implant facial bone following immediate implant placement and provisionalization of maxillary anterior single implants: A 1-year cone beam computed tomography study." *Int J Oral Maxillofac Implants* 2012; 27:393-400.
12. Patcas R, Muller L, Ullrich O, Peltomaki T. "Accuracy of cone-beam computed tomography at different resolutions assessed on the bony covering of the mandibular anterior teeth." *Am J Orthod Dentofacial Orthop* 2012; 141:41-50.
13. Ahlqvist JB, Isberg AM. "Validity of computed tomography in imaging thin walls of the temporal bone." *Dentomaxillofac Radiol* 1999; 28:13-19.
14. Miracle AC, Mukherji SK. "Conebeam CT of the head and neck, part 1: physical principles." *Am J Neuroradiol* 2009; 30:1088-1095.
15. Menezes CC, Janson G, Massaro CS, Cambiagli L, Garib DG. "Reproducibility of bone plate thickness measurements with cone-beam computed tomography using different image acquisition protocols." *Dental Press J Orthod* 2010; 15(5):143-149.
16. Sun Z, Smith T, Kortam S, Kim DG, Tee BC, et al. "Effect of bone thickness on alveolar bone-height measurements from cone-beam computed tomography images." *Am J Orthod Dentofacial Orthod* 2011; 139(2):e117-127.
17. Leung CC, Palomo L, Griffith R, & Hans MG. "Accuracy and reliability of cone-beam computed tomography for measuring alveolar bone height and detecting bony dehiscences and fenestrations." *Am J Orthod Dentofacial Orthod* 2010; 137(4):S109-119.
18. Hupp, Ellis, & Tucker, Eds. *Contemporary Oral and Maxillofacial Surgery, 5th ed.* St. Louis, 2008, Mosby-Elsevier.

Additional References

19. De Vos W, Casselman J, Swennen GRJ. "Cone-beam computerized tomography (CBCT) imaging of the oral and maxillofacial region: A systematic review of the literature." *Int J Oral Maxillofac Surg* 2009; 38:609-625.
20. Suomalainen A, Vehmas T, Kortensniemi M, Robinson S, Peltola J. "Accuracy of linear measurements using dental cone beam and conventional multislice computed tomography." *Dentomaxillofac Radiol* 2008; 37:10-17.
21. Timock AM, Cook V, McDonald T, Leo MC, Crowe J, et al. "Accuracy and reliability of buccal bone height and thickness measurements from cone-beam

- computed tomography imaging.” *Am J Orthod Dentofacial Orthod* 2011; 140(5):734-744.
22. Mol A & Balasundaram A. “In vitro cone beam computed tomography imaging of periodontal bone.” *Dentomaxillofac Radiol* 2008; 37:319-324.
 23. Docquier PL, Paul L, Cartiaux O, Lecouvet F, Dufrane D, et al. “Formalin fixation could interfere with the clinical assessment of the tumor-free margin in tumor surgery: magnetic resonance imaging-based study.” *Oncology* 2010; 78:115-124.
 24. Comert A, Kokat AM, Akkocaoglu M, Tekdemir I, Akca K, et al. “Fresh frozen vs. embalmed bone: is it possible to use formalin-fixed human bone for biomechanical experiments on implants?” *Clin Oral Implants Res* 2009; 20:521-525.
 25. Hansen P, Hassenkam T, Svensson RB, Aagaard P, Trappe T, et al. “Glutaraldehyde cross-linking of tendon—mechanical effects at the level of the tendon fascicle and fibril.” *Connect Tissue Res* 2009; 50:211-222.
 26. Burn-Murdoch RA, Tyler DW. “Physiological evidence that periodontal collagen in the rat exists as fibres prior to histological fixation.” *Arch Oral Biol* 1981; 26:995-999.